ARCHIVIO ISTITUZIONALE
DELLA RICERCA

Alma Mater Studiorum Università di Bologna
Archivio istituzionale della ricerca

Early appearance of developmental alterations in the dendritic tree of the hippocampal granule cells in the Ts65Dn model of Down syndrome

This is the final peer-reviewed author's accepted manuscript (postprint) of the following publication:

Published Version:
Uguagliati, B., Al-Absi, A.-R., Stagni, F., Emili, M., Giacomini, A., Guidi, S., et al. (2021). Early appearance of developmental alterations in the dendritic tree of the hippocampal granule cells in the Ts65Dn model of Down syndrome. HIPPOCAMPUS, 31(4), 435-447 [10.1002/hipo.23303].

Availability:
This version is available at: https://hdl.handle.net/11585/817344 since: 2025-06-30

Published:

DOI: http://doi.org/10.1002/hipo.23303

Terms of use:

Some rights reserved. The terms and conditions for the reuse of this version of the manuscript are specified in the publishing policy. For all terms of use and more information see the publisher's website.

This item was downloaded from IRIS Università di Bologna (https://cris.unibo.it/).
When citing, please refer to the published version.

(Article begins on next page)

17 September 2026

Title: Early appearance of developmental alterations in the dendritic tree of the hippocampal granule cells in the Ts65Dn model of Down syndrome

Authors: Beatrice Uguagliati [1], Abdel-Rahman Al-Absi [2], Fiorenza Stagni [3], Marco Emili [1], Andrea Giacomini [1], Sandra Guidi [1], Jens Randel Nyengaard [2*], Renata Bartesaghi [1*]

* Jens Randel Nyengaard and Renata Bartesaghi should be considered joint senior author.

Address:

1) Department of Biomedical and Neuromotor Sciences, University of Bologna, Bologna, Italy
2) Core Centre for Molecular Morphology, Section for Stereology and Microscopy, Department of Clinical Medicine, Aarhus University, Denmark
3) Department for Life Quality Studies, University of Bologna, Rimini, Italy

Running Title: Dendritic pattern in Ts65Dn pups

Corresponding author:
Prof. RENATA BARTESAGHI
Department of Biomedical and Neuromotor Sciences, Physiology Building
Piazza di Porta San Donato 2
I-40126 BOLOGNA BO, Italy
Tel +39 051 2091727
E-mail renata.bartesaghi@unibo.it

Co-Corresponding author:
Prof. JENS RANDEL NYENGAARD
Department of Clinical Medicine
C112
Palle Juul-Jensens Boulevard 35,
8200 Aarhus N, Denmark
Tel +4578469928
E-Mail jrnyengaard@clin.au.dk

ACKNOWLEDGMENT

This work was supported by a grant to R. B. from “Fondazione Generali e Assicurazione Generali”, Italy.

ABSTRACT

Down syndrome (DS), a genetic condition caused by triplication of chromosome 21, is characterized by alterations in various cognitive domains, including hippocampus-dependent memory functions, starting from early life stages. The major causes of intellectual disability in DS are prenatal neurogenesis alterations followed by impairment of dendritic development in early infancy. While there is evidence that the Ts65Dn mouse, the most widely used model of DS, exhibits dendritic alterations in adulthood, no studies are available regarding the onset of dendritic pathology. The goal of the current study was to establish whether this model exhibits early dendritic alterations in the hippocampus, a region whose function is severely damaged in DS. To this purpose, in Golgi-stained brains, we evaluated the dendritic arborization and dendritic spines of the granule cells of the hippocampal dentate gyrus in Ts65Dn mice aged 8 (P8) and 15 (P15) days. While P15 Ts65Dn mice exhibited a notably hypotrophic dendritic arbor and a reduced spine density, P8 mice exhibited a moderate reduction in the number of dendritic ramifications and no differences in spine density in comparison with their euploid counterparts. Both in P8 and P15 mice, spines were longer and had a longer neck, suggesting possible alterations in synaptic function. Moreover, P8 and P15 Ts65Dn mice had more thin spines and fewer stubby spines in comparison with euploid mice. Our study provides novel evidence on the onset of dendritic pathology, one of the causes of intellectual disability in DS, showing that it is already detectable in the dentate gyrus of Ts65Dn pups. This evidence strengthens the suitability of this model of DS as a tool to study dendritic pathology in DS and to test the efficacy of early therapeutic interventions aimed at ameliorating hippocampal development and, therefore, memory functions in children with DS.

Key words: Down syndrome; Ts65Dn model; hippocampus; granule neurons; dendritic pathology

INTRODUCTION

Damage of hippocampal development is a central feature of several genetic and neurodevelopmental disorders, including Down syndrome (DS) (Li, Shen, Stockton, & Zhao, 2019). DS is a relatively high-incidence genetic condition (prevalence: 1/700-1200 live birth) caused by triplication of chromosome 21. It is characterized by functional alterations in numerous cognitive domains, including hippocampus-dependent memory functions (Chapman & Hesketh, 2000; Vicari, 2004, 2006).

Accumulating evidence shows that in individuals with DS neurogenesis and cellularity are reduced in numerous brain regions, including the hippocampus, starting from fetal life stages (A Contestabile et al., 2007; Guidi et al., 2008; Guidi, Ciani, Bonasoni, Santini, & Bartesaghi, 2011; Stagni, Giacomini, Emili, Guidi, & Bartesaghi, 2018). Together with neurogenesis impairment, dendritic hypotrophy appears to be a second major cause of intellectual disability in DS (see (Bartesaghi, Guidi, & Ciani, 2011)). Unlike neurogenesis alterations, that take place prenatally, dendritic pathology begins to appear in infants starting from 3-4 months of age (L. E. Becker, Armstrong, & Chan, 1986; Prinz, Prinz, & Schulz, 1997; Schulz & Scholz, 1992; Takashima, Becker, Armstrong, & Chan, 1981). Likewise, while in the cortex of fetuses with DS spine counts are similar to those of control fetuses, new born and older infants with DS have a decreased number of spines (Takashima et al., 1981). In addition, starting from infancy spines are small, have short stalks and are intermingled with unusually long spines (Marin-Padilla, 1976; Purpura, 1979; Takashima et al., 1981). Thus, two fundamental processes of brain development, neurogenesis and dendritic maturation, are disrupted starting from the beginning of brain development, although dendritic alterations appear slightly later than neurogenesis alterations.

Numerous mouse models of DS have been created in order to identify the molecular mechanisms underlying DS and devise possible therapeutic interventions (Herault et al., 2017). Among these models, the Ts65Dn mouse represents the more widely used model because it replicates numerous features of DS. In particular, the Ts65Dn mouse exhibits neurogenesis alterations and dendritic pathology (see (Bartesaghi et al., 2011)), impairment of hippocampal long-term potentiation (LTP) (Begenisic et al., 2014; Costa & Grybko, 2005; Kleschevnikov, Belichenko, Faizi, et al., 2012), and reduced levels of performance in tasks that require the integrity of the hippocampal system (Demas, Nelson, Krueger, & Yarowsky, 1996; Faizi et al., 2011). In

view of its phenotypes mimicking DS, the Ts65Dn mouse has been largely employed in studies aimed at devising pharmacological interventions (see (K. J. Gardiner, 2015; Stagni, Giacomini, Guidi, Ciani, & Bartesaghi, 2015; Vacca et al., 2019)) potentially applicable to individuals with DS. In this connection, it must be emphasized that in view of the time course of dendritic development and the postnatal appearance of dendritic defects in infants with DS, the neonatal period may be a window of opportunity to improve neuronal maturation. Unfortunately, there is a strikingly paucity of studies that have characterized in depth the time-course of dendritic alterations in the hippocampus (and other brain regions) of individuals with DS and even fewer studies in the Ts65Dn model. It is known that the granule cells of the hippocampal dentate gyrus of Ts65Dn mice exhibit defects in dendritic complexity and dendritic spine density in adulthood (Belichenko et al., 2004; Dang et al., 2014; Guidi et al., 2013; F. Stagni et al., 2015) and that these defect are already present in mice aged 15 days (Emili et al., 2020; Stagni et al., 2017; Stagni et al., 2019). The onset of these defects, however, remains to be established. This knowledge is of obvious importance for the identification of the optimum time window for pharmacotherapies targeted to dendritic development. Based on these premises, the first goal of the current study was to establish whether defects in dendritic complexity and spine density are already present in the hippocampus of Ts65Dn pups aged eight days, an age at which dendritic spines begin to appear (Yuste & Bonhoeffer, 2004). In addition to defects in spine density, individuals with DS exhibit alterations in spine morphology (Marin-Padilla, 1976; Purpura, 1979), which most likely underlie alterations in synaptic communications. Defects in the spine morphology of the granule cells have been reported in adult Ts65Dn mice (Belichenko et al., 2004) but it is not known whether these defects are present at the beginning of hippocampal development. Therefore, the second goal of our study was to establish whether the dendritic spines of the granule cells of Ts65Dn mice already exhibit alterations in their morphology at the beginning of hippocampal development.

METHODS

Colony

Ts65Dn mice were generated by mating B6EiC3Sn a/ A-Ts(17^16)65Dn females with C57BL/6JEiJ x C3H/HeSnJ (B6EiC3Sn) F1 hybrid males. This parental generation was provided by Jackson Laboratories

(Bar Harbor, ME, USA). To maintain the original genetic background, the mice used here were of the first generation. Animals were genotyped as previously described (Reinholdt et al., 2011). The day of birth was designated postnatal day zero (P0). The animals' health and comfort were controlled by the veterinary service. The animals had access to water and food ad libitum and lived in a room with a 12:12h light/dark cycle. Experiments were performed in accordance with the European Communities Council Directive of 24 November 1986 (86/609/EEC) for the use of experimental animals and were approved by the Italian Ministry of Public Health (205/2019-PR). In this study, all efforts were made to minimize animal suffering and to keep the number of animals used to a minimum.

Experimental protocol

Euploid and Ts65Dn male mice were killed at postnatal day 8 (P8) and 15 (P15). The P15 mice were the same used in a previous study (Emili et al., 2020). Additional P15 mice were used for the study of spine morphology. The body weight was recorded prior to euthanization. The brains were excised, weighed, cut along the midline and the right hemisphere was processed for Golgi staining. The number of animals used for each experimental procedure is specified in the figure legends.

Histological procedures

Brains were Golgi stained using the FD Rapid Golgi Stain TM Kit (FD NeuroTechnologies, Inc.). The right hemispheres were immersed in the impregnation solution of the FD Rapid Golgi Stain TM Kit containing mercuric chloride, potassium dichromate and potassium chromate and were stored at room temperature in the dark for 2 weeks. Hemispheres were then transferred into Solution C of the same kit and stored at room temperature in the dark for at least 72h. After these steps, hemispheres were cut with a cryostat in 150-µm-thick coronal sections. Sections were mounted on super frost slides and air dried at room temperature in the dark for one day. After drying, sections were rinsed with distilled water and subsequently stained in a developing solution (FD Rapid Golgi Stain Kit) and coverslipped with DPX mounting medium.

Equipment

For the measurements of the dendritic tree and spine density we used a light microscope (Leitz) equipped with a motorized stage and focus control system and a Coolsnap-Pro color digital camera (Media Cybernetics, Silver Spring, MD, USA). Measurements were carried out using the software Image Pro Plus (Media Cybernetics, Silver Spring, MD 20910, USA). The images for 3D spine reconstruction were acquired using a light

microscope (Olympus BX50, Olympus, Denmark) equipped with a motorized stage (Prior scientific), a microcator (ND281, Heidenhain, Germany) and VIS Software (newCAST version 4.4.5.0. Visiopharm, Denmark). 3D reconstruction was performed using Imaris software (version 7.6.3) and a MATLAB (R2014a) dependent extension was used to classify dendritic spine morphology in distinguished classes.

Measurements

Measurement of the dendritic tree. The dendritic tree of the granule cells was traced with a dedicated custom-designed software for dendritic reconstruction (Immagini Computer di Maurizio Abbate & C. SNC, Bareggio, MI, Italy) interfaced with Image Pro Plus. The dendritic tree was traced live, at a final magnification of 500X, by focusing into the depth of the section. The operator starts with branches emerging from the cell soma and after having drawn the first parent branch goes on with all daughter branches of the next order in a centrifugal direction. At the end of tracing, the program reconstructs the total dendritic length, the number of branches of each order, and the mean length of branches of each order.

Spine density. Spines of granule cells of the dentate gyrus were counted live using a 100X oil immersion objective lens (Leitz microscope and objective with 1.4 NA). Spine density was evaluated in dendritic segments of distal dendrites, located in the outer half of the molecular layer. For each animal, spines were counted in at least 4/5 neurons, for a total of 15 segments per animal. The length of each sampled dendritic segment was determined by tracing its profile and the number of spines was counted manually. The linear spine density was calculated by dividing the total number of spines by the length of the dendritic segment. Spine density was expressed as number of spines per 100 μm dendrite.

Automatic spine reconstruction. Images of the dentate gyrus were acquired at 4X magnification (Fig. 1A). After delineating the region of interest in the dentate gyrus, granule neurons were selected (eight per animal) for 3D reconstruction using a 60X oil immersion lens, and with a Z-navigator. Once the Z-stack was created, the 3D reconstruction was initiated by processing the Z-stack with the Imaris software (Fig. 1B). To start spine reconstruction, a three-channel image was converted to a single channel image (green) (Fig. 1C). A global background subtraction was applied to all the images, in order to identify the object of interest against the background. For each neuron, four distal dendrites branches were traced with the "Autodepth" tool in Imaris surpass mode. Thereafter, spines were reconstructed with the automatic method (Fig. 1D). The software automatically generates a series of seed points along the dendritic branch. The seed points that did not represent

spines were excluded by setting the seed points threshold at an appropriate value. Imaris (Xtension), a MATLAB (R2014a) dependent extension, was used to classify dendritic spine morphology in one of four distinguished classes, i.e. filopodia, thin, mushroom and stubby (Fig. 1F-G; Table 1), as previously described (Al-Absi, Christensen, Sanchez, & Nyengaard, 2018). We evaluated the percentage of spines of each class and the following morphological parameters: spine length, neck length, neck volume, head volume, spine area. Spine parameters were evaluated by pooling together all spine classes.

Statistical analysis. Results are presented as mean ± standard error of the mean (SE). Data were analyzed with the IBM SPSS 22.0 software. Before running statistical analyses, we checked data distribution and homogeneity of variances for each variable using the Shapiro-Wilk test and Levene's test, respectively. If the data were normally distributed and variance was homogeneous, statistical analysis was carried out using either two tailed Student's t-test or a two-way ANOVA with genotype (euploid, Ts65Dn) and age (P8-P15), as factors. Post hoc multiple comparisons were carried out after two-way ANOVA using Fisher's least significant difference (LSD) test. If the data were not normally distributed and variance was heterogeneous, transformations were made to achieve normality. If the transformed data did not achieve normality, statistical analysis was carried out using either the Mann–Whitney U test or the Kruskal-Wallis test followed by the Mann–Whitney U test. Based on the "Box plot" tool available in SPSS Descriptive Statistics, in each analysis we excluded the extremes, i.e., values that were larger than 3 times the IQ range [$x \geq Q3+3 * (IQ)$; $x \leq Q1-3 * (IQ)$]. The number of mice included in (and excluded from, if any) individual analyses is reported in the legends of figs. A probability level of $p \leq 0.05$ was considered to be statistically significant.

RESULTS

Dendritic morphology of the granule cells in P8 Ts65Dn and euploid mice

In order to establish whether defects in dendritic morphology are already present at the earliest phases of hippocampal development, we examined the dendritic tree of the granule neurons in P8 Ts65Dn mice. We first examined the number of segments and the total length of the dendritic tree. A Student's t test showed that Ts65Dn mice had a reduced number of dendritic branches (-16%) compared to euploid mice [t=2.753; p=0.02]

(Fig. 2B) and a marginally significant reduction (-16%) in total dendritic length [t=2.162; p=0.056] (Fig. 2C). In order to analyze dendritic morphology in detail we examined each dendritic order separately. Regarding the number of dendritic branches of individual orders, we found no significant differences in the number of branches of each order although, in absolute terms, the number of ramifications in Ts65Dn mice was lower compared to euploid mice, starting from order 3 (Fig. 2D). Regarding the mean length of dendritic branches of individual orders, we found no differences between euploid and Ts65Dn mice (Fig. 2E). Taken together, these results show early appearing defects in the dendritic architecture of the granule cells of Ts65Dn mice, represented by an overall reduction in the number of dendritic branches and a trend to total dendritic length reduction.

Spine density of the granule cells in P8 Ts65Dn and euploid mice

Spine density reduction is a typical feature of the dendritic pathology that affects the brain of infants with DS (Takashima et al., 1981). Defects in spine density have been also observed in the dentate gyrus of the Ts65Dn mouse model aged 15 days (Emili et al., 2020; Stagni et al., 2017; Stagni et al., 2019). There is no information, however, regarding the onset of this defect. To this purpose, we examined the number of spines on the dendrites of granule neurons in P8 mice. The Mann-Whitney U test on spine density showed no differences between P8 Ts65Dn and euploid mice, indicating that during the early establishment of dendritic spines (Yuste & Bonhoeffer, 2004) there are no genotype-related differences in their density (Fig. 3B).

Comparison of the granule cell dendritic arbor in P8 and P15 Ts65Dn and euploid mice

Physiologically, development of the dendritic tree consists in regressive phenomena taking place during the early phases of neuron maturation. While the number of branches undergoes a reduction, there is a concomitant increase in dendritic length, which leads to an increase in total dendritic length. Most of the granule cells of the dentate gyrus are adult-like by day 14 (Jones, Rahimi, O'Boyle, Diaz, & Claiborne, 2003; Rihn & Claiborne, 1990). Therefore, we deemed it of interest to compare the dendritic architecture of P8 euploid and Ts65Dn mice with our previous data on the dendritic architecture of euploid and Ts65Dn mice aged 15 days, an age at which numerous defects are present in Ts65Dn mice (Emili et al., 2020). We first compared the number of segments and the total length of the dendritic tree. A two way ANOVA on the total

number of segment showed no genotype x age interaction, a main effect of genotype [$F(1,17)=18.586$, $p<0.001$], and a main effect of age [$F(1,17)=11.546$, $p=0.004$]. A *post hoc* Fisher's LSD test showed that P8 euploid mice had a larger number of dendritic ramifications compared to P15 euploid mice (+25%). An age-related difference also occurred in Ts65Dn mice that had a notably larger number of dendritic segments at P8 than at P15 (+40%) (Fig. 4A). At both ages, Ts65Dn mice had fewer branches than euploid mice. This difference increased with age being -16% in P8 Ts65Dn vs P8 euploid mice and –34% in P15 Ts65Dn vs P15 euploid mice (Fig. 4A). A two way ANOVA on the total length of the dendritic tree showed no genotype x age interaction, a main effect of genotype [$F(1,17)=24.546$, $p<0.001$] and a main effect of age [$F(1,17)=48.426$, $p=0.004$]. A *post hoc* Fisher's LSD test showed that P15 euploid mice had a total dendritic length larger that P8 euploid mice (+21%) while there was no length increase in P15 Ts65Dn mice in comparison with P8 Ts65Dn mice (Fig. 4B). At both ages, Ts65Dn had a reduced dendritic length in comparison with euploid mice. This difference increased with age being -16% in P8 Ts65Dn vs P8 euploid mice and –26% in P15 Ts65Dn vs P15 euploid mice (Fig. 4B).

In order to compare the dendritic architecture of P8 and P15 mice in detail, we examined the total number of segments (Fig. 4C) and the mean segment length (Fig. 4D) of each dendritic order separately. The total number of segments of order 1 could not be statistically evaluated because all groups had a single primary dendrite. The Kruskal-Wallis test on the number of segments of order 1 showed no significant effects. A two-way ANOVA on the number of segments of order 3 showed no genotype x age interaction, a main effect of genotype [$F(1,17)=7.100$, $p=0.016$], and a main effect of age [$F(1,17)=20.568$, $p<0.001$]. A *post hoc* Fisher's LSD test showed that both euploid and Ts65Dn mice aged 8 days had more dendritic branches than their counterparts aged 15 days. A two-way ANOVA on the number of segment of order 4 showed no genotype x age interaction, a main effect of genotype [$F(1,17)=21.583$, $p<0.001$], and a main effect of age [$F(1,17)=23.709$, $p<0.001$]. A *post hoc* Fisher's LSD test showed that both euploid and Ts65Dn mice aged 8 days had more dendritic branches than their counterparts aged 15 days, although the difference between P8 and P15 euploid mice was marginally significant only ($p=0.053$). A two-way ANOVA on the number of segment of order 5 showed no genotype x age interaction, a main effect of genotype [$F(1,17)=7.006$, $p=0.017$], and a main effect of age [$F(1,17)=19.124$, $p<0.001$]. A *post hoc* Fisher's LSD test showed that both euploid and Ts65Dn mice aged 8 days had more dendritic branches than their counterparts aged 15 days. The Kruskal-Wallis test

on the number of segments of order 6 showed no significant effects.

A two-way ANOVA on the length of segments of order 1 showed a genotype x age interaction [$F(1,17)=14.259$, $p=0.002$], a main effect of genotype [$F(1,17) = 8.841$, $p=0.009$], and a main effect of age [$F(1,17)=8.766$, $p<0.001$]. A *post hoc* Fisher's LSD test showed no age-related length difference for euploid mice. In contrast, P15 Ts65Dn mice had a greater dendritic length compared to P8 Ts65Dn mice. A two-way ANOVA on the length of segments of order 2 showed a genotype x age interaction [$F(1,17)=4.992$, $p=0.002$], a main effect of genotype [$F(1,17)=7.208$, $p=0.016$], and a main effect of age [$F(1,17) = 47.904$, $p<0.001$]. A *post hoc* Fisher's LSD test showed that both euploid and Ts65Dn mice aged 15 days had a greater dendritic length than their counterparts aged 8 days. A two-way ANOVA on the length of segments of order 3 showed no genotype x age interaction, no main effect of genotype, and a main effect of age [$F(1,16)=89.67$, $p<0.001$]. A *post hoc* Fisher's LSD test showed that both euploid and Ts65Dn mice aged 15 days had a greater dendritic length than their counterparts aged 8 days. A two-way ANOVA on the length of segment of order 4 showed a genotype x age interaction [$F(1,15)=7.357$, $p=0.015$], no main effect of genotype, and a main effect of age [$F(1,17)=76.737$, $p<0.001$]. A *post hoc* Fisher's LSD test showed that both euploid and Ts65Dn mice aged 15 days had a greater dendritic length than their counterparts aged 8 days. A two-way ANOVA on the length of segments of order 5 showed no genotype x age interaction, no main effect of genotype, and a main effect of age [$F(1,14)=15.131$, $p=0.002$]. A *post hoc* Fisher's LSD test showed that both euploid and Ts65Dn mice aged 15 days had a greater dendritic length than their counterparts aged 8 days. A two-way ANOVA on the length of segments of order 6 showed no genotype x age interaction, no main effect of genotype, and a main effect of age [$F(1,7)=15.279$, $p=0.006$]. Euploid mice aged 15 days had a greater dendritic length than their counterparts aged 8 days (Fig. 4D).

Taken together these results show that in both genotypes the total number of dendritic ramifications decreases with age. This effect is due to a reduction in the number of branches of order 3-5 in both genotypes and loss of branches of order 6 in P15 Ts65Dn mice. Observation of Fig. 4C shows that although the number of dendritic branches undergoes a regression both in euploid and Ts65Dn mice, the reduction in the branch number was larger in Ts65Dn mice. Regarding total dendritic length, euploid mice undergo an increase from P8 to 15, because although there is a regression of branches of order >2, the remaining branches undergo a notable length increase. In Ts65Dn mice, although there is an age-related increase in the length of branches of

all orders, total dendritic length does not undergo an increase because the increase in branch length is outweighed by reduction in the number of branches of order >2.

Comparison of dendritic spine density on the granule cells in P8 and P15 Ts65Dn and euploid mice

We compared spine density in P8 and P15 mice in order to establish whether, similarly to changes in dendritic complexity there are also early age-related spine density differences. A two-way ANOVA on spine density showed no genotype x age interaction, no main effect of age, but a main effect of genotype [$F(1,18)=7.022$, $p=0.016$]. A *post hoc* Fisher's LSD showed that P15 euploid mice had more dendritic spines compared to P8 euploid mice (+14%), while there was no difference in spine density between P8 and P15 Ts65Dn mice (Fig. 5). These results show that in euploid mice the number of dendritic spines on the granule cells of the dentate gyrus undergoes an age-related increase. On the contrary, spine density in Ts65Dn mice remains the same in P8 and P15 mice.

Size parameters of granule cell dendritic spines in P8 and P15 Ts65Dn and euploid mice

Several morphological parameters, such as spine length, neck and head size contribute to the stability and functionality of dendritic spines (Sala & Segal, 2014; Yuste & Bonhoeffer, 2004). Since there are no data regarding spine shape in Ts65Dn mice during the early stages of spine development, in the current study we analyzed some key morphological parameters of dendritic spines in P8 and P15 euploid and Ts65Dn mice.

The Kruskal-Wallis test on spine length showed a significant difference between groups [$\chi2$ (3) = 10.071, $p=0.018$]. The Mann-Whitney test showed that both in P8 and P15 Ts65Dn mice spine length was larger (+12 % at P8 and +15% at P15) compared to age-matched euploid mice (P8: $U=5$, $p=0.03$; P15: $U=5$, $p=0.037$) (Fig. 6A). Regarding the neck length, the Kruskal-Wallis test showed a significant difference between groups [$\chi2$ (3)=9.197, $p=0.027$]. The Mann-Whitney test demonstrated a longer neck (+18%) in P8 Ts65Dn mice compared to P8 euploid mice ($U=4$, $p=0.025$) (Fig. 6B). A two way ANOVA on neck volume showed no genotype x age interaction, no main effect of age, but a main effect of genotype [$F(1,20)=4.387$, $p=0.049$]. A *post hoc* Fisher's LSD showed that in P8 Ts65Dn mice neck volume was larger in comparison with P8 (+100%) and P15 (+74%) euploid mice (Fig. 6C). The statistical analysis on head volume and spine area showed no differences between groups (Fig. 6D,E). Taken together these results show that P8 Ts65Dn

mice have spines with greater total length, a neck longer and with greater volume in comparison with P8 euploid mice and that the difference in total spine length is retained at P15.

Types of granule cell dendritic spines in P8 and P15 Ts65Dn and euploid mice

On the basis of their morphological characteristics dendritic spines are traditionally classified into four major categories: filopodia, thin, stubby, and mushroom (Fig. 1D) (Parnass, Tashiro, & Yuste, 2000). Though dendritic spines are prone to rapid morphological plasticity, spine classification can give a simplified snapshot of the dendritic spine population and their functionality. In order to establish whether there are differences in the relative number of the different spine types between euploid and Ts65Dn mice and whether those differences undergo changes over time, we analyzed the percentage of spines of each class in P8 and P15 mice.

The Kruskal-Wallis test showed no differences between groups in the percentage of filopodia (Fig. 7A). A two way ANOVA on the percentage of thin spines showed no genotype x age interaction, no main effect of age, but a main effect of genotype [$F(1,20)=8.694$, $p=0.008$]. A *post hoc* Fisher's LSD showed that P8 euploid mice had fewer thin spines compared to P8 (-21%) and P15 (-26%) Ts65Dn mice (Fig. 7B). P15 euploid mice also had fewer thin spines (-11%) in comparison with P15 Ts65Dn mice, although this difference was not statistically significant. The Kruskal-Wallis test showed no differences between groups in the percentage of mushroom spines (Fig. 7C). A two way ANOVA on the percentage of stubby spines showed no genotype x age interaction, a main effect of age [$F(1,20)=11.409$, $p=0.003$] and a main effect of genotype [$F(1,20)=8.937$, $p=0.007$]. A *post hoc* Fisher's LSD showed that P8 euploid mice had a higher percentage of stubby spines compared to P8 (+24%) and P15 (+64%) Ts65Dn mice. Similarly to P8 mice, P15 euploid mice had more stubby spines (+12%) in comparison with P15 Ts65Dn mice, although this difference was marginally significant (Fig. 7D). In addition, P15 euploid mice had fewer stubby spines than P8 (-21%) euploid mice and P15 Ts65Dn mice had fewer stubby spines compared to P8 Ts65Dn mice (-25%) (Fig. 7D). Taken together these results show that P8 and P15 Ts65Dn mice have a higher percentage of thin spines and fewer stubby spines compared to the euploid counterparts. The percentage of stubby spines decreases with age both in euploid and Ts65Dn mice.

DISCUSSION

The granule cells of Ts65Dn pups exhibit a reduced dendritic complexity that worsens with age

Evidence in fetuses and infants with DS shows that during gestation and the first months of life individual with DS exhibit a normal or even increased dendritic complexity compared to euploid children (L. E. Becker et al., 1986; Benavides-Piccione et al., 2004; Vuksic, Petanjek, Rasin, & Kostovic, 2002). Starting from the first year of age, however, children with DS exhibit a steady decrease in dendritic branching (L. E. Becker et al., 1986) that becomes more pronounced in adulthood (L. Becker, Mito, Takashima, & Onodera, 1991; Benavides-Piccione et al., 2004; Takashima, Ieshima, Nakamura, & Becker, 1989). In the current study, we provide novel information regarding the appearance of dendritic abnormalities in the dentate gyrus of the Ts65Dn mouse model of DS. We found that at the end of the first week of age the dendritic tree of the granule cells of Ts65Dn mice has a reduced number of branches and a marginally reduced length. An analysis of the number and length of branches of each order showed no differences between euploid and Ts65Dn mice. We previously found that by the end of the second week of age the granule cells of Ts65Dn mice had a notably reduced number of branches and total dendritic length, and fewer branches of orders 3-5 in comparison with euploid mice (Emili et al., 2020). This indicates that moderate defects in dendritic arbor are present at 8 days of age and that these defects worsen in the time-period of one week. These defects in dendritic complexity are retained during further stages of development and consequently adolescents and adult Ts65Dn mice have granule cells with a notably hypotrophic dendritic arbor in comparison with euploid mice (Belichenko et al., 2004; Dang et al., 2014; Guidi et al., 2013; F. Stagni et al., 2015).

Neurons eliminate excess dendritic branches giving origin to a mature arbor pattern that remains altogether stable once the animal reaches adulthood (Lefebvre, Sanes, & Kay, 2015). A comparison of the dendritic tree of P8 an P15 mice showed a reduced number of ramifications in P15 mice, independently from the genotype. The age-related reduction in the number of dendritic branches, however, was larger in Ts65Dn mice (see Fig. 4A,C), suggesting an early-occurring excessive pruning of the dendritic tree. In parallel with elimination of dendritic branches, there was an increase in the length of branches of the different orders, in both euploid and Ts65Dn mice (Fig. 4D). While in euploid mice the length increase outweighed the reduction in the number of branches and, consequently, there was an age-related increase in total dendritic length (Fig.

4B), a similar effect did not occur in Ts65Dn mice that at P15 had a dendritic length similar to that at P8. The local activation of caspase is required for elimination of dendritic branches in mammalian neurons (Lefebvre et al., 2015). Increased activation/expression of cleaved caspase-3 has been detected in the brain of fetuses and adults with DS (Guidi et al., 2008; Stadelmann et al., 1999) and in the Ts65Dn mouse model (Bianchi, Ciani, Contestabile, Guidi, & Bartesaghi, 2010), suggesting that this increase may be a factor contributing to excessive dendritic pruning.

The granule cells of Ts65Dn pups have normal dendritic spine density but spine density decreases with age

A study in fetuses with DS reported no differences in spine shapes and density compared to age matched euploid fetuses (Takashima et al., 1989). However, in newborn and infants with DS a reduced spine density and the presence of unusually short and thin spines as well as "hair like" dendritic spines have been observed (Marin-Padilla, 1976; Purpura, 1975; Suetsugu & Mehraein, 1980; Takashima et al., 1989). In the present study, we observed that Ts65Dn mice aged 8 days had a similar number of spines on granule cell dendrites as P8 euploid mice. In contrast, P15 Ts65Dn mice have a reduced spine density in comparison with their euploid counterparts (Emili et al., 2020). A comparison of spine density in P8 and P15 mice of the same genotype showed that while in euploid mice spine density increases with age, in P15 Ts65Dn mice spine density remains the same as in P8 mice (see Fig. 5). Studies in adult mice report a reduced spine density in the dentate gyrus of Ts65Dn mice compared to euploid mice of the same age (Belichenko et al., 2004; Guidi et al., 2014; F. Stagni et al., 2015). This evidence indicates a failure of dendritic spine growth in Ts65Dn mice and that this defect is retained across life. Defects in spine development/pruning characterize different developmental disorders (Penzes, Cahill, Jones, VanLeeuwen, & Woolfrey, 2011). It remains to be established whether the developing brain of Ts65Dn mice (and individuals with DS) is affected by lack of new spines formation or whether newborn spines are extensively pruned.

Aberrant shape of granule cell dendritic spines in Ts65Dn pups

The analysis of spine morphological parameters is fundamental in order to understand spine function and stability (Parnass et al., 2000). The study of different parameters of spine head and neck can give

information about dendritic spine function, including the abundance of receptors, diffusion of small molecules between spine and shaft, as well as the motility and stability of the spine (Lai & Ip, 2013).

We found that the spines of P8 and P15 Ts65Dn were longer in comparison with those of euploid mice. In addition, in P8 Ts65Dn mice spines had a neck that was longer and had a larger volume compared to euploid mice. The presence of the spine neck is fundamental for synaptic activity (Lai & Ip, 2013). The length of the neck is inversely correlated with synaptic efficacy (Araya, Vogels, & Yuste, 2014), suggesting that the long spine neck in Ts65Dn mice may contribute to impaired synaptic signaling in the dentate gyrus. In infants with DS, dendritic spines have a typically elongated shape, although very large dendritic spines with prominent heads can also be observed (Marin-Padilla, 1976). Accordingly, we found here that in Ts65Dn pups most of the dendritic spines of the granule cells had an elongated shape. This is in contrast with evidence that in P21 and older Ts65Dn mice granule neurons have a relatively large number of spines with abnormally large head and short neck (Belichenko et al., 2004). It has been suggested that the size of the spine head is inversely related to the strength of excitatory input signals (Murthy, Schikorski, Stevens, & Zhu, 2001). Mouse models of DS present reduced excitatory drive and enhanced GABAergic activity, especially in the hippocampal formation (A. Contestabile, Magara, & Cancedda, 2017; Giacomini et al., 2015; Guidi et al., 2013; Hanson, Blank, Valenzuela, Garner, & Madison, 2007; Kleschevnikov, Belichenko, Gall, et al., 2012; Stagni et al., 2016). Thus, improper organization of excitatory and inhibitory inputs during hippocampal development may account for the increase in spine head size found in adolescent and adult Ts65Dn mice (Belichenko et al., 2004).

Dendritic spines are highly dynamic structures and their rapid creation, destruction and remodeling are essential for brain plasticity. For simplicity, however, dendritic spines are often classified into four classes: filopodia, thin, stubby, and mushroom, according to spine shape (Berry & Nedivi, 2017; Ghani et al., 2017; Parnass et al., 2000). The classification under a determinate class could give an indication about spine maturation, stability and functioning. An analysis of the percentage of the different spine types showed that both P8 and P15 Ts65Dn mice had a higher percentage of thin spines compared to euploid mice and fewer stubby spines. Interestingly, similar defects have been observed in CA1 apical dendrites on adult Ts65Dn mice (Day et al., 2019). We found, in addition, that in Ts65Dn and euploid mice the percentage of stubby spines decreased with age. No genotype- or age-related difference were found in the percentage of filopodia and

mushroom spines. Stubby spines are small protrusions emerging from the dendrite, usually very abundant during early development (Harris, Jensen, & Tsao, 1992), while thin spines are dynamic structures, that can be formed or removed within hours, often associated with learning (Berry & Nedivi, 2017). The abundance of thin spines in Ts65Dn mice observed here may indicate an effort to counteract defects in learning-related synaptic plasticity. A study in primary cultures of cortical neurons from Ts65Dn pups found no difference in spine density in comparison with euploid mice, and a decrease in the density of long neck spines (possibly corresponding to our thin spines) and of mushroom spines at 14 days in vitro (Chiotto et al., 2019). The discrepancy between our current data and those obtained by Belichenko (Belichenko et al., 2004) vs. those obtained by Chiotto et al. may be due to the different types of examined neurons (cortical neurons in the study by Chiotto et al.) or the simplified conditions of *in vitro* systems, where neurons lack afferent signals.

The molecular mechanisms underlying dendritic spine defects in DS are not well understood although some triplicated genes are likely to be involved in dendritic spine dismorphogenesis and reduced density. Among these genes, DSCR1 (Down syndrome critical region1; also called RCAN1, regulator of calcineurin) and DYRK1A (dual-specificity tyrosine-phosphorylation-regulated kinase 1A) may be of particular relevance because their increased expression in mice recapitulates some phenotypes of DS, including alterations in spine density and shape (S. Lee, H, & Webb, 2015). Among the genes located on HSA21 there are several genes that encode receptors for interferons (IFN) (Ferrando-Miguel et al., 2003). Recent evidence shows that thrombospondin-1, a protein secreted by astrocytes which is fundamental for spinogenesis, is reduced in the Ts65Dn mouse and DS brains and that this defect is due to upregulation of IFN-γ signaling (Torres, Garcia, Tang, & Busciglio, 2018). In addition to triplication of Chromosome 21 genes, individuals with DS exhibit overexpression of Chromosome 21 miR-155, miR-802, miR-125b-2, let-7c, and miR-99a (Siew, Tan, Babaei, Cheah, & Ling, 2013). Overexpression of miR-155 and miR-802 has been also documented in in Ts65Dn mice. Both miR-155 and miR-802 target the methyl CpG binding protein2 (MeCP2) (Siew et al., 2013). Loss of MeCP2 function causes Rett syndrome and results in abnormal dendritic spine morphology and decreased dendritic arbor complexity and spine density (Armstrong, 2005). Thus, miR-induced downregulation of MeCP2 in DS (Keck-Wherley et al., 2011) may also contribute to alter the development of dendritic spines and dendrites.

No information is available regarding spine type distribution in fetuses and adults with DS. The abundant thin spine observed here in the dentate gyrus of neonate Ts65Dn mice could correspond to the unusually long thin and "hair like" spines described in children with DS (Marin-Padilla, 1976; Purpura, 1973). Although it is known that spine density is reduced in the DS brain, a systematic analysis of spine types in different brain regions, neuron populations and at different ages is missing. Such an analysis is fundamental to validate data obtained in different mouse models of DS and help understand the impact of synaptic pathology in the DS brain.

Significance

The Ts65Dn mouse, which is trisomic for a segment of mouse chromosome 16 that is orthologous to the long arm of human chromosome 21 (K. Gardiner, Fortna, Bechtel, & Davisson, 2003)) is the more widely used model of DS because it exhibits numerous features mimicking those of individuals with DS. The drawback of this model is that it also carries three copies of an extra segment (arising from Mmu17) with non-DS-related genes (Herault et al., 2017), which may contribute to its phenotype. Ts1Cje mice and Ts1Rhr mice are only trisomic for a shorter segment of mouse chromosome 16 in comparison with Ts65Dn mice (Herault et al., 2017). Importantly, they show alterations in dendritic spine density and dendritic complexity in the dentate gyrus resembling those seen in the Ts65Dn mouse (Belichenko, Kleschevnikov, Salehi, Epstein, & Mobley, 2007:Belichenko, 2009 #2529), suggesting that the dendritic features of Ts65Dn mice are not due to triplication of their extra segment.

The architecture of the dendritic arbor has implications in brain information processing, determining the number, position and type of synapses a given neuron will have and shaping circuits formation (Lefebvre et al., 2015). Dendritic spines, that are the major component of excitatory synapses, have a modulatory role in synaptic transmission and neuronal functioning (K. F. Lee, Soares, & Béïque, 2012). Number, shape and dynamics of dendritic spines reflect the strength of synapses (Benavides-Piccione et al., 2004; Maiti, Manna, Ilavazhagan, Rossignol, & Dunbar, 2015). We found here numerous defects in the dendritic development of the granule cells of Ts65Dn mice (summarized in Table 2) and that the dendritic arbor of the granule neurons of Ts65Dn mice already exhibits a reduced number of branches in pups aged 8 days. Concomitant with dendritic size reduction, we found alterations in spine morphology, with an aberrant increase in total spine and neck length. Although there were no differences in the percentage of filopodia and mushroom spines, defined

as immature and mature spines respectively, the imbalance in the percentage of stubby and thin spines observed in Ts65Dn during early development indicates an early defect of spinogenesis and spine maturation in this mouse model of DS. The granule cells of the dentate gyrus are the first element of the hippocampal trisynaptic circuit (granule cells-field CA3 pyramidal neurons-field CA1 pyramidal neurons) that plays a fundamental role in long-term learning and memory. Correct synaptic functioning in the dentate gyrus is prerequisite for further signal processing along the hippocampal network. Taken together, the current findings show that dendritic pathology, one of the main causes of intellectual disability in DS, is detectable in the dentate gyrus of Ts65Dn pups. This evidence strengthens the suitability of this widely used mouse model of DS as a tool to exploit early therapeutic interventions aimed at ameliorating hippocampal development and therefore intellectual disability in children with DS.

CONFLICT OF INTEREST

The authors declare that they have no conflict of interest.

AUTHORSHIP

BU Carried out histology, analyzed spine parameters and dendritic arborization, and was involved in drafting the manuscript. AA Analyzed spine parameters. FS Carried out histology and was involved in drafting the manuscript. ME Analyzed dendritic arborization and spine density. AG Carried out statistical analysis and prepared the figures. SG Carried out histology and was involved in drafting the manuscript. JRN Supervised evaluation of spine parameters and was involved in drafting the manuscript. RB Conceived the study and wrote the article.

DATA AVAILABILITY

The data that support the findings of this study are available from the corresponding author upon reasonable request.

REFERENCES

Al-Absi, A. R., Christensen, H. S., Sanchez, C., & Nyengaard, J. R. (2018). Evaluation of semi-automatic 3D reconstruction for studying geometry of dendritic spines. J Chem Neuroanat, 94, 119-124. doi:10.1016/j.jchemneu.2018.10.008

Araya, R., Vogels, T. P., & Yuste, R. (2014). Activity-dependent dendritic spine neck changes are correlated with synaptic strength. *Proceedings of the National Academy of Sciences of the United States of America, 111*(28), E2895-2904. doi:10.1073/pnas.1321869111

Armstrong, D. D. (2005). Neuropathology of Rett syndrome. *J Child Neurol, 20*(9), 747-753. doi:10.1177/08830738050200090901

Bartesaghi, R., Guidi, S., & Ciani, E. (2011). Is it possible to improve neurodevelopmental abnormalities in Down syndrome? *Rev Neurosci, 22*(4), 419-455. doi:10.1515/RNS.2011.037

Becker, L., Mito, T., Takashima, S., & Onodera, K. (1991). Growth and development of the brain in Down syndrome. *Prog Clin Biol Res, 373*, 133-152. Retrieved from http://www.ncbi.nlm.nih.gov/entrez/query.fcgi?cmd=Retrieve&db=PubMed&dopt=Citation&list_uids=1838182

Becker, L. E., Armstrong, D. L., & Chan, F. (1986). Dendritic atrophy in children with Down's syndrome. *Ann Neurol, 20*(4), 520-526. doi:10.1002/ana.410200413

Begenisic, T., Baroncelli, L., Sansevero, G., Milanese, M., Bonifacino, T., Bonanno, G., . . . Sale, A. (2014). Fluoxetine in adulthood normalizes GABA release and rescues hippocampal synaptic plasticity and spatial memory in a mouse model of Down syndrome. *Neurobiology of disease, 63*, 12-19. doi:10.1016/j.nbd.2013.11.010

Belichenko, P. V., Kleschevnikov, A. M., Salehi, A., Epstein, C. J., & Mobley, W. C. (2007). Synaptic and cognitive abnormalities in mouse models of Down syndrome: exploring genotype-phenotype relationships. *J Comp Neurol, 504*(4), 329-345. doi:10.1002/cne.21433

Belichenko, P. V., Masliah, E., Kleschevnikov, A. M., Villar, A. J., Epstein, C. J., Salehi, A., & Mobley, W. C. (2004). Synaptic structural abnormalities in the Ts65Dn mouse model of Down Syndrome. *J Comp Neurol, 480*(3), 281-298. doi:10.1002/cne.20337

Benavides-Piccione, R., Ballesteros-Yanez, I., de Lagran, M. M., Elston, G., Estivill, X., Fillat, C., . . . Dierssen, M. (2004). On dendrites in Down syndrome and DS murine models: a spiny way to learn. *Prog Neurobiol, 74*(2), 111-126. doi:10.1016/j.pneurobio.2004.08.001

Berry, K. P., & Nedivi, E. (2017). Spine Dynamics: Are They All the Same? *Neuron, 96*(1), 43-55. doi:10.1016/j.neuron.2017.08.008

Bianchi, P., Ciani, E., Contestabile, A., Guidi, S., & Bartesaghi, R. (2010). Lithium restores neurogenesis in the subventricular zone of the Ts65Dn mouse, a model for Down syndrome. *Brain Pathol, 20*(1), 106-118. doi:10.1111/j.1750-3639.2008.00246.x

Chapman, R. S., & Hesketh, L. J. (2000). Behavioral phenotype of individuals with Down syndrome. *Ment Retard Dev Disabil Res Rev, 6*(2), 84-95. doi:10.1002/1098-2779(2000)6:2<84::AID-MRDD2>3.0.CO;2-P

Chiotto, A. M. A., Migliorero, M., Pallavicini, G., Bianchi, F. T., Gai, M., Di Cunto, F., & Berto, G. E. (2019). Neuronal Cell-Intrinsic Defects in Mouse Models of Down Syndrome. *Frontiers in neuroscience, 13*, 1081. doi:10.3389/fnins.2019.01081

Contestabile, A., Fila, T., Ceccarelli, C., Bonasoni, P., Bonapace, L., Santini, D., . . . Ciani, E. (2007). Cell cycle alteration and decreased cell proliferation in the hippocampal dentate gyrus and in the neocortical germinal matrix of fetuses with Down syndrome and in Ts65Dn mice. *Hippocampus, 17*(8), 665-678. doi:10.1002/hipo.20308

Contestabile, A., Magara, S., & Cancedda, L. (2017). The GABAergic Hypothesis for Cognitive Disabilities in Down Syndrome. *Front Cell Neurosci, 11*, 54. doi:10.3389/fncel.2017.00054

Costa, A. C., & Grybko, M. J. (2005). Deficits in hippocampal CA1 LTP induced by TBS but not HFS in the Ts65Dn mouse: a model of Down syndrome. *Neurosci Lett, 382*(3), 317-322. doi:10.1016/j.neulet.2005.03.031

Dang, V., Medina, B., Das, D., Moghadam, S., Martin, K. J., Lin, B., . . . Salehi, A. (2014). Formoterol, a long-acting beta2 adrenergic agonist, improves cognitive function and promotes dendritic complexity in a mouse model of Down syndrome. *Biol Psychiatry, 75*(3), 179-188. doi:10.1016/j.biopsych.2013.05.024

Day, S. M., Yang, W., Wang, X., Stern, J. E., Zhou, X., Macauley, S. L., & Ma, T. (2019). Glucagon-Like Peptide-1 Cleavage Product Improves Cognitive Function in a Mouse Model of Down Syndrome. *eNeuro, 6*(2). doi:10.1523/ENEURO.0031-19.2019

Demas, G. E., Nelson, R. J., Krueger, B. K., & Yarowsky, P. J. (1996). Spatial memory deficits in segmental trisomic Ts65Dn mice. *Behav Brain Res, 82*(1), 85-92. doi:10.1016/s0166-4328(97)81111-4

Emili, M., Stagni, F., Salvalai, M. E., Uguagliati, B., Giacomini, A., Albac, C., . . . Guidi, S. (2020). Neonatal therapy with clenbuterol and salmeterol restores spinogenesis and dendritic complexity in the dentate gyrus of the Ts65Dn model of Down syndrome. *Neurobiology of disease, 140*, 104874. doi:10.1016/j.nbd.2020.104874

Faizi, M., Bader, P. L., Tun, C., Encarnacion, A., Kleschevnikov, A., Belichenko, P., . . . Shamloo, M. (2011). Comprehensive behavioral phenotyping of Ts65Dn mouse model of Down syndrome: activation of beta1-adrenergic receptor by xamoterol as a potential cognitive enhancer. *Neurobiology of disease, 43*(2), 397-413. doi:10.1016/j.nbd.2011.04.011

Ferrando-Miguel, R., Shim, K. S., Cheon, M. S., Gimona, M., Furuse, M., & Lubec, G. (2003). Overexpression of Interferon α/β Receptor β Chain in Fetal Down Syndrome Brain. *Neuroembryology and Aging, 2*(4), 147-155. doi:10.1159/000079401

Gardiner, K., Fortna, A., Bechtel, L., & Davisson, M. T. (2003). Mouse models of Down syndrome: how useful can they be? Comparison of the gene content of human chromosome 21 with orthologous mouse genomic regions. *Gene, 318*, 137-147. doi:10.1016/s0378-1119(03)00769-8

Gardiner, K. J. (2015). Pharmacological approaches to improving cognitive function in Down syndrome: current status and considerations. *Drug Des Devel Ther, 9*, 103-125. doi:10.2147/DDDT.S51476

Ghani, M. U., Mesadi, F., Kanık, S. D., Argunşah, A., Hobbiss, A. F., Israely, I., . . . Çetin, M. (2017). Dendritic spine classification using shape and appearance features based on two-photon microscopy. *J Neurosci Methods, 279*, 13-21. doi:10.1016/j.jneumeth.2016.12.006

Giacomini, A., Stagni, F., Trazzi, S., Guidi, S., Emili, M., Brigham, E., . . . Bartesaghi, R. (2015). Inhibition of APP gamma-secretase restores Sonic Hedgehog signaling and neurogenesis in the Ts65Dn mouse model of Down syndrome. *Neurobiology of disease, 82*, 385-396. doi:10.1016/j.nbd.2015.08.001

Guidi, S., Bonasoni, P., Ceccarelli, C., Santini, D., Gualtieri, F., Ciani, E., & Bartesaghi, R. (2008). Neurogenesis impairment and increased cell death reduce total neuron number in the hippocampal region of fetuses with Down syndrome. *Brain Pathol, 18*(2), 180-197. doi:10.1111/j.1750-3639.2007.00113.x

Guidi, S., Ciani, E., Bonasoni, P., Santini, D., & Bartesaghi, R. (2011). Widespread Proliferation Impairment and Hypocellularity in the Cerebellum of Fetuses with Down Syndrome. *Brain Pathol, 21*, 361-373. doi:10.1111/j.1750-3639.2010.00459.x

Guidi, S., Stagni, F., Bianchi, P., Ciani, E., Giacomini, A., De Franceschi, M., . . . Bartesaghi, R. (2014). Prenatal pharmacotherapy rescues brain development in a Down's syndrome mouse model. *Brain, 137*(Pt 2), 380-401. doi:10.1093/brain/awt340

Guidi, S., Stagni, F., Bianchi, P., Ciani, E., Ragazzi, E., Trazzi, S., . . . Bartesaghi, R. (2013). Early pharmacotherapy with fluoxetine rescues dendritic pathology in the Ts65Dn mouse model of Down syndrome. *Brain Pathol, 23*(2), 129-143. doi:10.1111/j.1750-3639.2012.00624.x

Hanson, J. E., Blank, M., Valenzuela, R. A., Garner, C. C., & Madison, D. V. (2007). The functional nature of synaptic circuitry is altered in area CA3 of the hippocampus in a mouse model of Down's syndrome. *J Physiol, 579*(Pt 1), 53-67. doi:10.1113/jphysiol.2006.114868

Harris, K. M., Jensen, F. E., & Tsao, B. (1992). Three-dimensional structure of dendritic spines and synapses in rat hippocampus (CA1) at postnatal day 15 and adult ages: implications for the maturation of synaptic physiology and long-term potentiation. *The Journal of neuroscience : the official journal of the Society for Neuroscience, 12*(7), 2685-2705. doi:10.1523/jneurosci.12-07-02685.1992

Herault, Y., Delabar, J. M., Fisher, E. M. C., Tybulewicz, V. L. J., Yu, E., & Brault, V. (2017). Rodent models in Down syndrome research: impact and future opportunities. *Dis Model Mech, 10*(10), 1165-1186. doi:10.1242/dmm.029728

Jones, S. P., Rahimi, O., O'Boyle, M. P., Diaz, D. L., & Claiborne, B. J. (2003). Maturation of granule cell dendrites after mossy fiber arrival in hippocampal field CA3. *Hippocampus, 13*(3), 413-427. doi:10.1002/hipo.10121

Keck-Wherley, J., Grover, D., Bhattacharyya, S., Xu, X., Holman, D., Lombardini, E. D., . . . Galdzicki, Z. (2011). Abnormal microRNA expression in Ts65Dn hippocampus and whole blood: contributions to Down syndrome phenotypes. *Dev Neurosci, 33*(5), 451-467. doi:10.1159/000330884

Kleschevnikov, A. M., Belichenko, P. V., Faizi, M., Jacobs, L. F., Htun, K., Shamloo, M., & Mobley, W. C. (2012). Deficits in cognition and synaptic plasticity in a mouse model of Down syndrome ameliorated by GABAB receptor antagonists. *The Journal of neuroscience : the official journal of the Society for Neuroscience, 32*(27), 9217-9227. doi:10.1523/JNEUROSCI.1673-12.2012

Kleschevnikov, A. M., Belichenko, P. V., Gall, J., George, L., Nosheny, R., Maloney, M. T., . . . Mobley, W. C. (2012). Increased efficiency of the GABAA and GABAB receptor-mediated neurotransmission in the Ts65Dn mouse model of Down syndrome. *Neurobiology of disease, 45*(2), 683-691. doi:10.1016/j.nbd.2011.10.009

Lai, K. O., & Ip, N. Y. (2013). Structural plasticity of dendritic spines: the underlying mechanisms and its dysregulation in brain disorders. *Biochimica et biophysica acta, 1832*(12), 2257-2263. doi:10.1016/j.bbadis.2013.08.012

Lee, K. F., Soares, C., & Béïque, J. C. (2012). Examining form and function of dendritic spines. *Neural plasticity, 2012*, 704103. doi:10.1155/2012/704103

Lee, S., H, Z., & Webb, D. (2015). Dendritic spine morphology and dynamics in health and disease.

. *Cell Health and Cytoskeleton, 7*, 121-131. doi:https://doi.org/10.2147/CHC.S82214

Lefebvre, J. L., Sanes, J. R., & Kay, J. N. (2015). Development of dendritic form and function. *Annu Rev Cell Dev Biol, 31*, 741-777. doi:10.1146/annurev-cellbio-100913-013020

Li, Y., Shen, M., Stockton, M. E., & Zhao, X. (2019). Hippocampal deficits in neurodevelopmental disorders. *Neurobiol Learn Mem, 165*, 106945. doi:10.1016/j.nlm.2018.10.001

Maiti, P., Manna, J., Ilavazhagan, G., Rossignol, J., & Dunbar, G. L. (2015). Molecular regulation of dendritic spine dynamics and their potential impact on synaptic plasticity and neurological diseases. *Neurosci Biobehav Rev, 59*, 208-237. doi:10.1016/j.neubiorev.2015.09.020

Marin-Padilla, M. (1976). Pyramidal cell abnormalities in the motor cortex of a child with Down's syndrome. A Golgi study. *J Comp Neurol, 167*(1), 63-81. doi:10.1002/cne.901670105

Murthy, V. N., Schikorski, T., Stevens, C. F., & Zhu, Y. (2001). Inactivity produces increases in neurotransmitter release and synapse size. *Neuron, 32*(4), 673-682. doi:10.1016/s0896-6273(01)00500-1

Parnass, Z., Tashiro, A., & Yuste, R. (2000). Analysis of spine morphological plasticity in developing hippocampal pyramidal neurons. *Hippocampus, 10*(5), 561-568. doi:10.1002/1098-1063(2000)10:5<561::AID-HIPO6>3.0.CO;2-X

Penzes, P., Cahill, M. E., Jones, K. A., VanLeeuwen, J. E., & Woolfrey, K. M. (2011). Dendritic spine pathology in neuropsychiatric disorders. *Nat Neurosci, 14*(3), 285-293. doi:10.1038/nn.2741

Prinz, M., Prinz, B., & Schulz, E. (1997). The growth of non-pyramidal neurons in the primary motor cortex of man: a Golgi study. *Histol Histopathol, 12*(4), 895-900. Retrieved from

http://www.ncbi.nlm.nih.gov/entrez/query.fcgi?cmd=Retrieve&db=PubMed&dopt=Citation&list_uids=9302548

Purpura, D. P. (1973). Normal and aberrant development of synaptic pathways in human hippocampus. *Trans Am Neurol Assoc, 98*, 224-226. Retrieved from http://www.ncbi.nlm.nih.gov/entrez/query.fcgi?cmd=Retrieve&db=PubMed&dopt=Citation&list_uids=4274161

Purpura, D. P. (1975). Normal and aberrant neuronal development in the cerebral cortex of human fetus and young infant. *UCLA Forum Med Sci*(18), 141-169. doi:10.1016/b978-0-12-139050-1.50014-8

Purpura, D. P. (1979). Pathobiology of cortical neurons in metabolic and unclassified amentias. *Res Publ Assoc Res Nerv Ment Dis, 57*, 43-68. Retrieved from http://www.ncbi.nlm.nih.gov/entrez/query.fcgi?cmd=Retrieve&db=PubMed&dopt=Citation&list_uids=217050

Reinholdt, L. G., Ding, Y., Gilbert, G. J., Czechanski, A., Solzak, J. P., Roper, R. J., . . . Davisson, M. T. (2011). Molecular characterization of the translocation breakpoints in the Down syndrome mouse model Ts65Dn. *Mamm Genome, 22*(11-12), 685-691. doi:10.1007/s00335-011-9357-z

Rihn, L. L., & Claiborne, B. J. (1990). Dendritic growth and regression in rat dentate granule cells during late postnatal development. *Brain Res Dev Brain Res, 54*(1), 115-124. doi:10.1016/0165-3806(90)90071-6

Sala, C., & Segal, M. (2014). Dendritic spines: the locus of structural and functional plasticity. *Physiol Rev, 94*(1), 141-188. doi:10.1152/physrev.00012.2013

Schulz, E., & Scholz, B. (1992). [Neurohistological findings in the parietal cortex of children with chromosome aberrations]. *J Hirnforsch, 33*(1), 37-62. Retrieved from http://www.ncbi.nlm.nih.gov/entrez/query.fcgi?cmd=Retrieve&db=PubMed&dopt=Citation&list_uids=1447516

Siew, W. H., Tan, K. L., Babaei, M. A., Cheah, P. S., & Ling, K. H. (2013). MicroRNAs and intellectual disability (ID) in Down syndrome, X-linked ID, and Fragile X syndrome. *Front Cell Neurosci, 7*, 41. doi:10.3389/fncel.2013.00041

Stadelmann, C., Deckwerth, T. L., Srinivasan, A., Bancher, C., Bruck, W., Jellinger, K., & Lassmann, H. (1999). Activation of caspase-3 in single neurons and autophagic granules of granulovacuolar degeneration in Alzheimer's disease. Evidence for apoptotic cell death. *Am J Pathol, 155*(5), 1459-1466. doi:10.1016/S0002-9440(10)65460-0

Stagni, F., Giacomini, A., Emili, M., Guidi, S., & Bartesaghi, R. (2018). Neurogenesis impairment: An early developmental defect in Down syndrome. *Free radical biology & medicine, 114*, 15-32. Retrieved from <Go to ISI>://MEDLINE:28756311

Stagni, F., Giacomini, A., Emili, M., Trazzi, S., Guidi, S., Sassi, M., . . . Bartesaghi, R. (2016). Short- and long-term effects of neonatal pharmacotherapy with epigallocatechin-3-gallate on hippocampal

development in the Ts65Dn mouse model of Down syndrome. *Neuroscience, 333*, 277-301. doi:10.1016/j.neuroscience.2016.07.031

Stagni, F., Giacomini, A., Guidi, S., Ciani, E., & Bartesaghi, R. (2015). Timing of therapies for Down syndrome: the sooner, the better. *Frontiers in behavioral neuroscience, 9*, 265. Retrieved from <Go to ISI>://MEDLINE:26500515

Stagni, F., Giacomini, A., Guidi, S., Ciani, E., Ragazzi, E., Filonzi, M., . . . Bartesaghi, R. (2015). Long-term effects of neonatal treatment with fluoxetine on cognitive performance in Ts65Dn mice. *Neurobiology of disease, 74C*, 204-218. doi:10.1016/j.nbd.2014.12.005

Stagni, F., Giacomini, A., Guidi, S., Emili, M., Uguagliati, B., Salvalai, M. E., . . . Bartesaghi, R. (2017). A flavonoid agonist of the TrkB receptor for BDNF improves hippocampal neurogenesis and hippocampus-dependent memory in the Ts65Dn mouse model of DS. *Exp Neurol, 298*(Pt A), 79-96. doi:10.1016/j.expneurol.2017.08.018

Stagni, F., Salvalai, M. E., Giacomini, A., Emili, M., Uguagliati, B., Xia, E., . . . Guidi, S. (2019). Neonatal treatment with cyclosporine A restores neurogenesis and spinogenesis in the Ts65Dn model of Down syndrome. *Neurobiology of disease, 129*, 44-55. doi:10.1016/j.nbd.2019.05.005

Suetsugu, M., & Mehraein, P. (1980). Spine distribution along the apical dendrites of the pyramidal neurons in Down's syndrome. A quantitative Golgi study. *Acta Neuropathol, 50*(3), 207-210. doi:10.1007/BF00688755

Takashima, S., Becker, L. E., Armstrong, D. L., & Chan, F. (1981). Abnormal neuronal development in the visual cortex of the human fetus and infant with down's syndrome. A quantitative and qualitative Golgi study. *Brain Res, 225*(1), 1-21. doi:10.1016/0006-8993(81)90314-0

Takashima, S., Ieshima, A., Nakamura, H., & Becker, L. E. (1989). Dendrites, dementia and the Down syndrome. *Brain Dev, 11*(2), 131-133. doi:10.1016/s0387-7604(89)80082-8

Torres, M. D., Garcia, O., Tang, C., & Busciglio, J. (2018). Dendritic spine pathology and thrombospondin-1 deficits in Down syndrome. *Free radical biology & medicine, 114*, 10-14. doi:10.1016/j.freeradbiomed.2017.09.025

Vacca, R. A., Bawari, S., Valenti, D., Tewari, D., Nabavi, S. F., Shirooie, S., . . . Nabavi, S. M. (2019). Down syndrome: Neurobiological alterations and therapeutic targets. *Neurosci Biobehav Rev, 98*, 234-255. doi:10.1016/j.neubiorev.2019.01.001

Vicari, S. (2004). Memory development and intellectual disabilities. *Acta Paediatr Suppl, 93*(445), 60-63; discussion 63-64. doi:10.1111/j.1651-2227.2004.tb03059.x

Vicari, S. (2006). Motor development and neuropsychological patterns in persons with Down syndrome. *Behav Genet, 36*(3), 355-364. doi:10.1007/s10519-006-9057-8

Vuksic, M., Petanjek, Z., Rasin, M. R., & Kostovic, I. (2002). Perinatal growth of prefrontal layer III pyramids in Down syndrome. *Pediatr Neurol, 27*(1), 36-38. doi:10.1016/s0887-8994(02)00380-6

Yuste, R., & Bonhoeffer, T. (2004). Genesis of dendritic spines: insights from ultrastructural and imaging studies. *Nat Rev Neurosci, 5*(1), 24-34. doi:10.1038/nrn1300

Table 1. Parameters of the different spine classes.

Spine Class	Classification criteria
Stubby	Length<0.5 μm
Mushroom	Length<1.26 μm and mean width head>mean width neck x1.2
Long thin	Min width head≥min width neck
Filopodia	None of the above

Table 2. Genotype and age effects on the granule cell dendrites in Ts65Dn and euploid mice.

	GENOTYPE EFFECT		AGE EFFECT	
	P8 mice	P15 mice	Eu mice	Ts mice
DENDRITIC ARBOR				
Number of segments	**Ts < Eu**	**Ts < Eu**	**P15 > P8**	**P15 > P8**
Total Length	**Ts < Eu ***	**Ts < Eu**	**P15 > P8**	P15 = P8
DENDRITIC SPINES				
Density	Ts = Eu	**Ts < Eu**	**P15 > P8**	P15 = P8
Spine length	**Ts > Eu**	**Ts > Eu**	P15 = P8	P15 = P8
Neck length	**Ts > Eu**	Ts = Eu	P15 = P8	P15 = P8
Neck volume	**Ts > Eu**	Ts = Eu	P15 = P8	P15 = P8
Head volume	Ts = Eu	Ts = Eu	P15 = P8	P15 = P8
Area	Ts = Eu	Ts = Eu	P15 = P8	P15 = P8
% of filopodia	Ts = Eu	Ts = Eu	P15 = P8	P15 = P8
% of thin spines	**Ts > Eu**	Ts = Eu	P15 = P8	P15 = P8
% of mushroom spines	Ts = Eu	Ts = Eu	P15 = P8	P15 = P8
% of stubby spines	**Ts < Eu**	**Ts < Eu ***	**P15 < P8**	**P15 < P8**

Summary of the comparisons of the dendritic tree and dendritic spines of the granule cells in euploid (Eu) and Ts65Dn (Ts) mice aged 8 (P8 mice) and 15 (P15 mice) days. The columns under the heading "Genotype effect" report the comparisons between Ts65Dn and euploid mice at P8 and P15, respectively, and the columns under the heading "Age effect" report the results of the comparisons between P8 and P15 mice of the same genotype. Significant differences are highlighted with bold characters. The asterisk indicates a marginal difference. See Results for major details.

FIGURE LEGENDS

Fig. 1. Dendritic spine reconstruction.

Example of a Golgi-stained brain section acquired at 4X magnification. Calibration bar=1000 μm. B: Granule cell acquired with a 60X immersion oil objective. Calibration bar=20 μm. C: Granule cell after Z-stack conversion to single channel image. Calibration bar=20 μm. D: Dendritic branch selected for 3D reconstruction. Calibration bar=2 μm. E, F: Dendritic spines (blue color) reconstructed with the automatic method. Calibration bar=2 μm. G: Schematic drawing of spines classified into four different classes. Abbreviations: CA1, hippocampal field; DG, dentate gyrus.

Fig. 2. Dendritic architecture of the granule cells of P8 Ts65Dn and euploid mice.

A: Examples of the reconstructed dendritic tree of two granule cells from the dentate gyrus of an euploid mouse and a Ts65Dn mouse. Numbers indicate the different dendritic orders. Calibration bar=20 μm. B-E: Total number of dendritic branches (B), total dendritic length (C), number (D) and mean length (E) of branches of the different orders of euploid (n=5) and Ts65Dn (n=7) mice. Values in B-E represent mean ± SE. (*) $p = 0.06$; * $p \leq 0.05$ (Student's t-test).

Fig. 3. Dendritic spine density on the granule cells of P8 Ts65Dn and euploid mice.

A: Photomicrographs of Golgi-stained granule cell dendrites showing spines on distal dendritic branches in a euploid and a Ts65Dn mouse. Calibration bar=4 μm. B: Spine density (mean ± SE) on the distal dendrites of the granule cells of euploid (n=6) and Ts65Dn (n=6) mice.

Fig. 4. Comparison of the dendritic architecture of P8 and P15 Ts65Dn and euploid mice.

A-D Total number of dendritic branches (A), total dendritic length (B), number (C) and mean length (D) of branches of the different orders of P8 euploid (n=5) and Ts65Dn (n=7) mice and P15 euploid (n=5) and Ts65Dn (n=4) mice. The lack of branches of order 6 in Ts65Dn mice is indicated by a black arrow. Values in A-D represent mean ± SE. (*) $p < 0.06$; * $p \leq 0.05$; ** $p \leq 0.01$; *** $p \leq 0.001$ (Fisher LSD test after two-way ANOVA or Mann-Whitney test after Kruskal-Wallis test). Abbreviation: Eu, euploid.

Fig. 5. Comparison of spine density on the granule cells of P8 and P15 Ts65Dn and euploid mice.

Spine density (mean ± SE) on the distal dendrites of the granule cells of P8 euploid (n=6) and Ts65Dn (n=6) mice and P15 euploid (n=6) and Ts65Dn (n=6) mice. * $p \leq 0.05$; ** $p \leq 0.01$ (Fisher LSD test after two-way ANOVA). Abbreviation: Eu, euploid.

Fig. 6. Comparison of granule cell spine parameters of P8 and P15 Ts65Dn and euploid mice.

A-E: Total spine length (A), neck length (B), neck volume (C), head volume (D), and spine surface are (E) of dendritic spines on the distal dendrites of P8 euploid (n=6) and Ts65Dn (n=6) mice and P15 euploid (n=6) and Ts65Dn (n=6) mice. * $p \leq 0.05$; ** $p \leq 0.01$ (Fisher LSD test after two-way ANOVA or Mann-Whitney test after Kruskal-Wallis test). Abbreviation: Eu, euploid.

Fig. 7. Comparison of spine types of P8 and P15 Ts65Dn and euploid mice.

A-D: Percentage of filopodia (A), thin spines (B), mushroom spines (C), and stubby spines (D) on the distal dendrites of P8 euploid (n=6) and Ts65Dn (n=6) mice and P15 euploid (n=6) and Ts65Dn (n=6) mice. (*) $p = 0.06$; * $p \leq 0.05$; ** $p \leq 0.01$; *** $p \leq 0.001$ (Fisher LSD test after two-way ANOVA or Mann-Whitney test after Kruskal-Wallis test). Abbreviation: Eu, euploid.

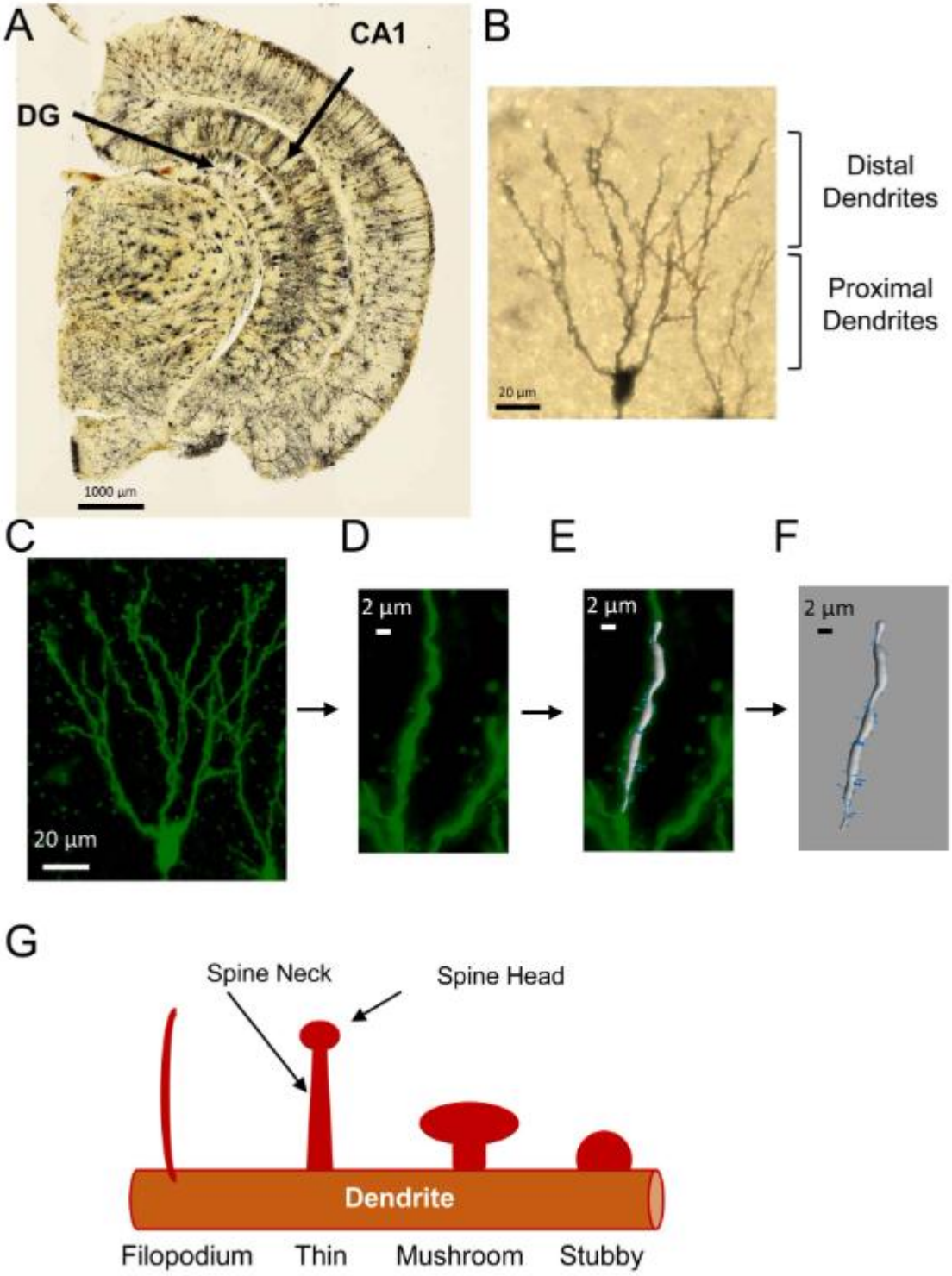
A
CA1
DG
1000 µm
B
Distal Dendrites
Proximal Dendrites
20 µm
C
20 µm
D
2 µm
E
2 µm
F
2 µm
G
Spine Neck
Spine Head
Dendrite
Filopodium
Thin
Mushroom
Stubby

1

2

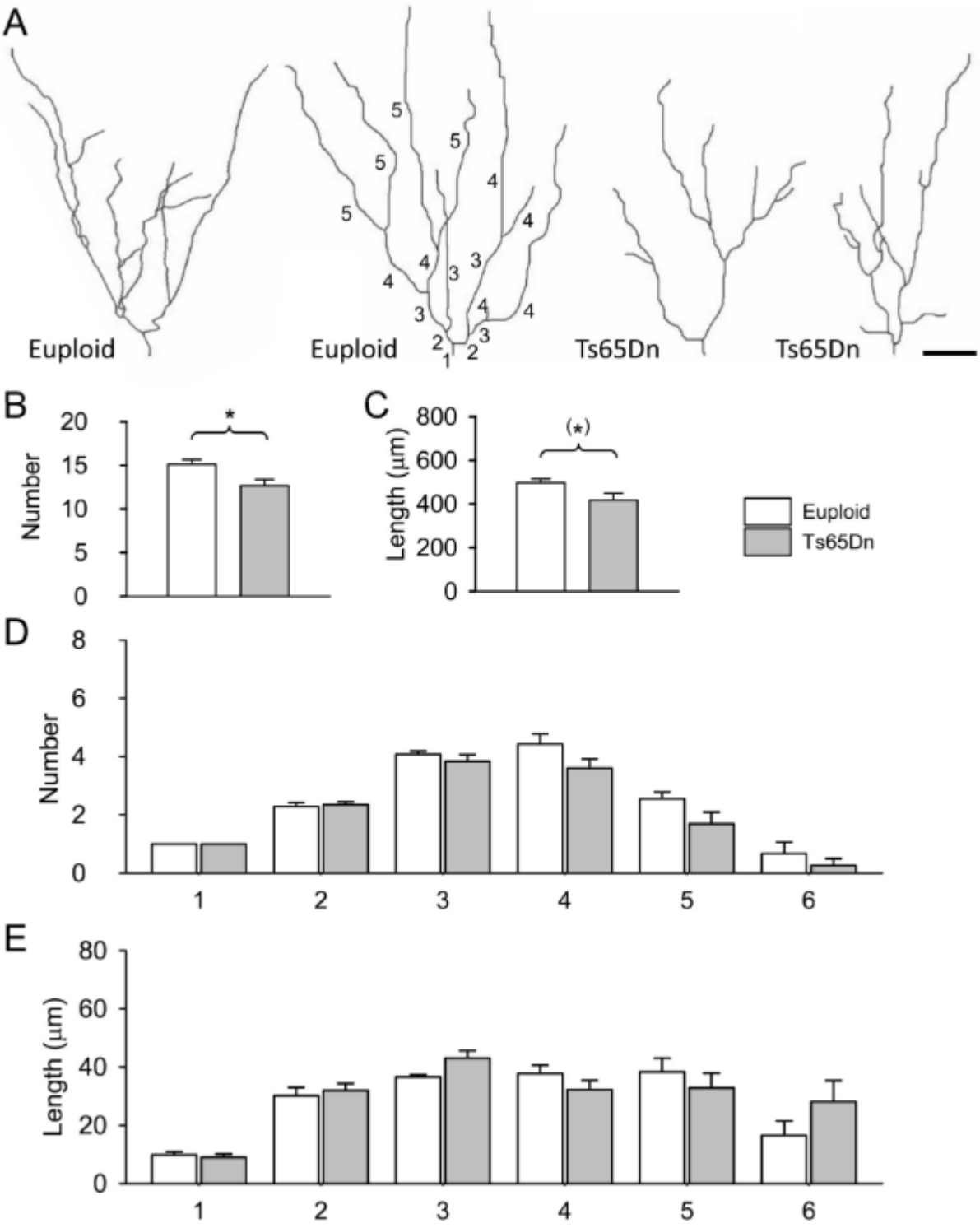
A
Euploid
Euploid
Ts65Dn
Ts65Dn
B
Number
20
15
10
5
0
*
C
Length (µm)
800
600
400
200
0
(*)
Euploid
Ts65Dn
D
Number
8
6
4
2
0
1
2
3
4
5
6
E
Length (µm)
80
60
40
20
0
1
2
3
4
5
6

1

2

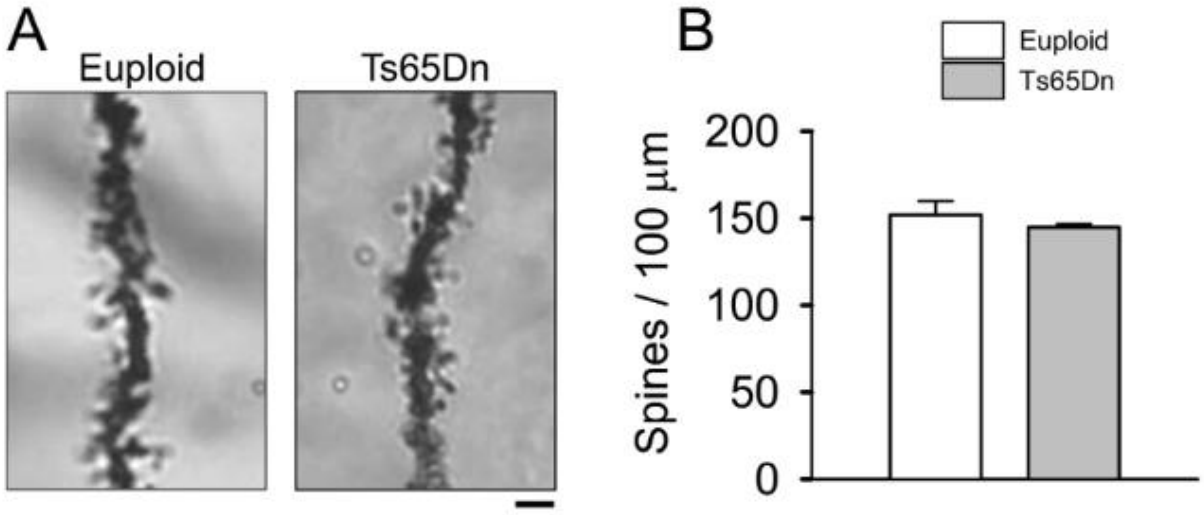
A
Euploid
Ts65Dn
B
Euploid
Ts65Dn
Spines / 100 µm
200
150
100
50
0

1

2

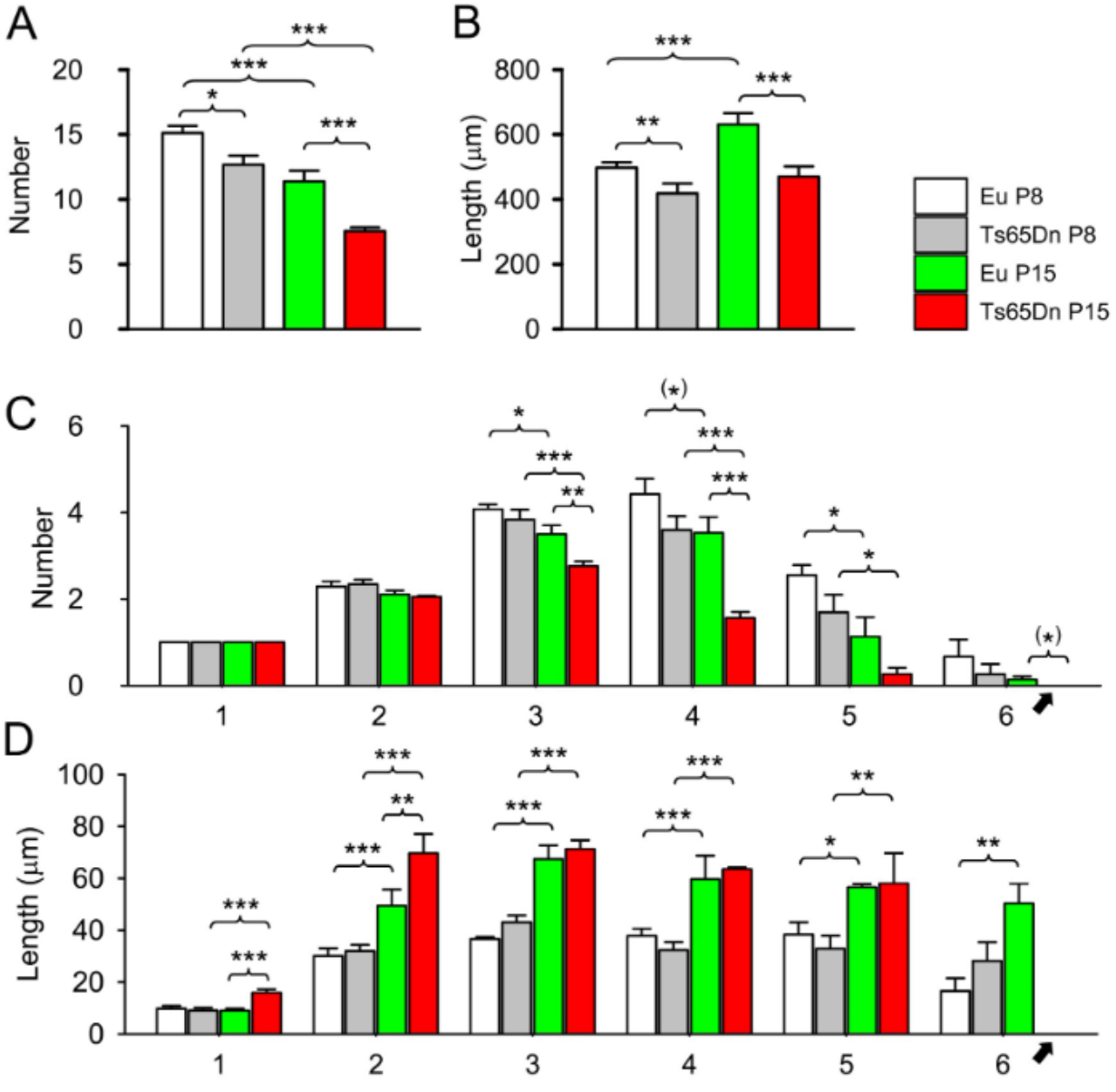
A
Number
20
15
10
5
0
*
***
***
***
B
Length (µm)
800
600
400
200
0
**
***
***
Eu P8
Ts65Dn P8
Eu P15
Ts65Dn P15
C
Number
6
4
2
0
*
***
**
(*)
***
***
*
*
(*)
1
2
3
4
5
6
D
Length (µm)
100
80
60
40
20
0
***
***
***
**
***
***
***
***
***
***
*
**
**
1
2
3
4
5
6

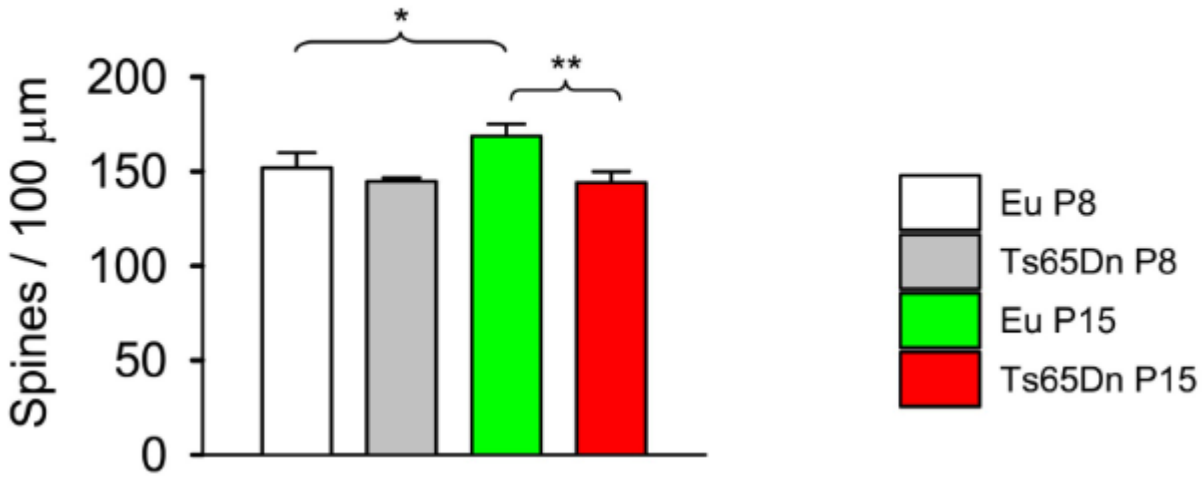

1

2

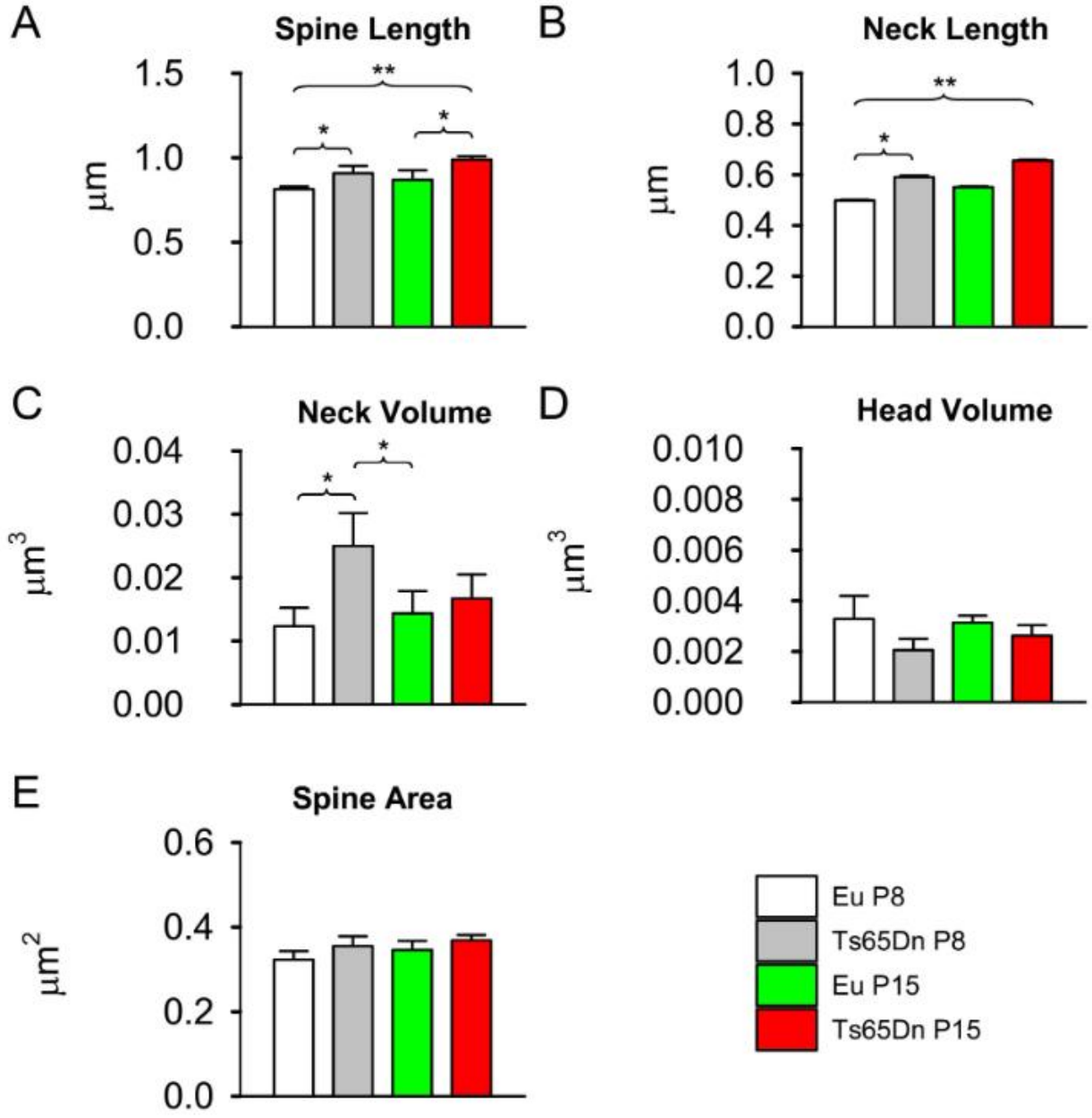
A
Spine Length
1.5
1.0
0.5
0.0
µm
**
*
*
B
Neck Length
1.0
0.8
0.6
0.4
0.2
0.0
µm
**
*
C
Neck Volume
0.04
0.03
0.02
0.01
0.00
µm3
*
*
D
Head Volume
0.010
0.008
0.006
0.004
0.002
0.000
µm3
E
Spine Area
0.6
0.4
0.2
0.0
µm2
Eu P8
Ts65Dn P8
Eu P15
Ts65Dn P15

1

2

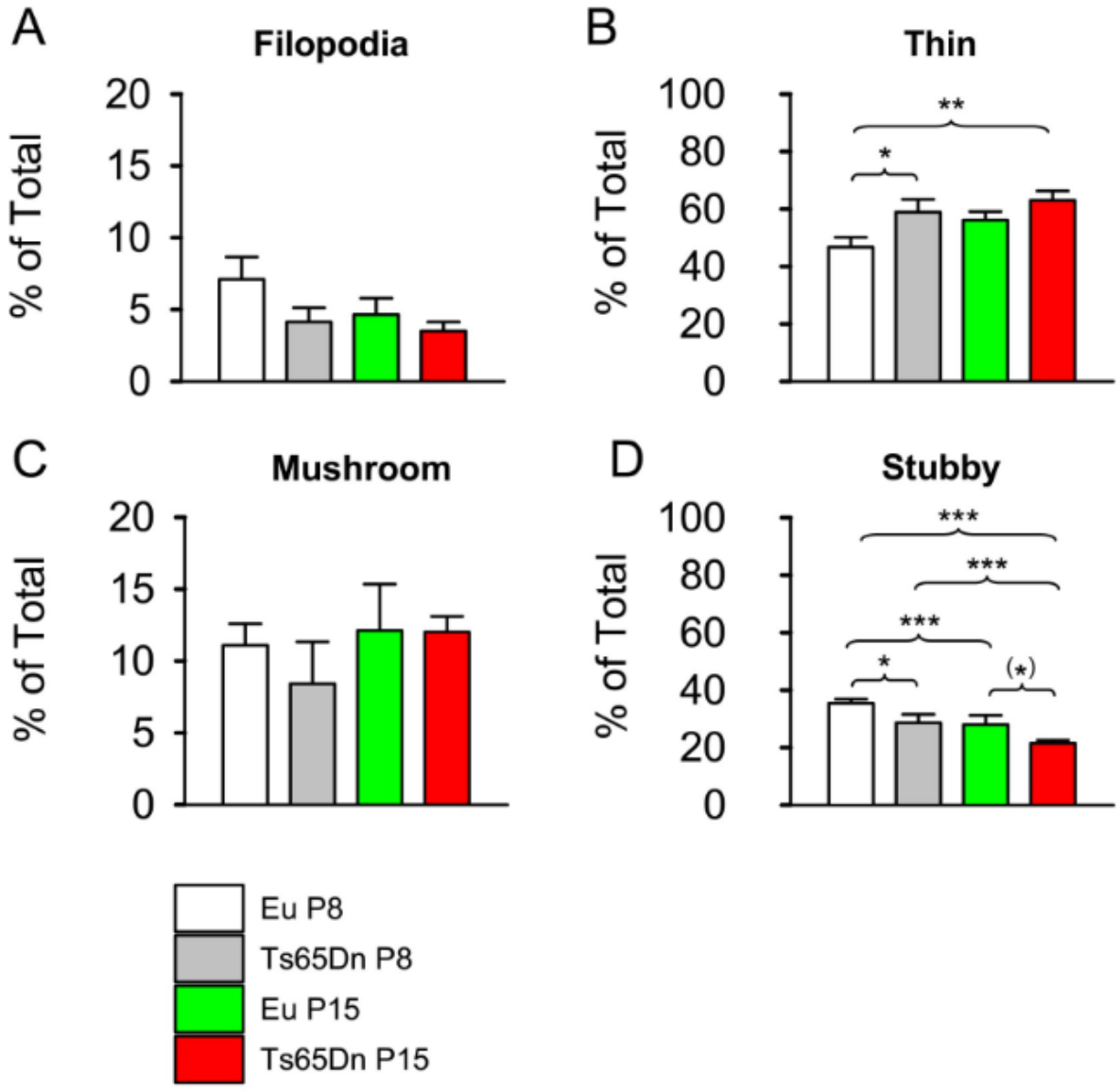
A
Filopodia
% of Total
20
15
10
5
0
B
Thin
% of Total
100
80
60
40
20
0
**
*
C
Mushroom
% of Total
20
15
10
5
0
D
Stubby
% of Total
100
80
60
40
20
0
***
***
***
*
(*)
Eu P8
Ts65Dn P8
Eu P15
Ts65Dn P15

1

2